

A Stealthy and Robust Fingerprinting Scheme for Generative Models

Li Guanlin

Nanyang Technological University
guanlin001@e.ntu.edu.sg

Guo Shangwei

Chongqing University
gswei5555@gmail.com

Wang Run

Wuhan University
wangrun@whu.edu.cn

Xu Guowen

Nanyang Technological University
guowen.xu@ntu.edu.sg

Zhang Tianwei

Nanyang Technological University
tianwei.zhang@ntu.edu.sg

Abstract

This paper presents a novel fingerprinting methodology for the Intellectual Property protection of generative models. Prior solutions for discriminative models usually adopt adversarial examples as the fingerprints, which give anomalous inference behaviors and prediction results. Hence, these methods are not stealthy and can be easily recognized by the adversary. Our approach leverages the invisible backdoor technique to overcome the above limitation. Specifically, we design verification samples, whose model outputs look normal but can trigger a backdoor classifier to make abnormal predictions. We propose a new backdoor embedding approach with Unique-Triplet Loss and fine-grained categorization to enhance the effectiveness of our fingerprints. Extensive evaluations show that this solution can outperform other strategies with higher robustness, uniqueness and stealthiness for various GAN models.

1. Introduction

Generative models aim to produce new data samples following certain distributions or requirements. One popular solution is Generative Adversarial Networks (GANs) [10], which is based on the contest between two neural networks. A generator network tries to fabricate new samples indistinguishable from real samples, while a discriminator network aims to identify the difference between them. Such contest drives the generator to produce high-quality and realistic data. State-of-the-art GAN algorithms and techniques have been commonly used in many computer vision applications, e.g., image synthesis [35], attribute editing [15], photo implanting [8], image-to-image translation [25], etc.

Training a production-level GAN model requires a large amount of resources, valuable data, and human expertise. Therefore, a well-trained GAN model (especially the generator) has become the core Intellectual Property (IP) of AI

applications. It is important to protect such assets, and prevent illegitimate plagiarism, unauthorized distribution and reproduction of GAN models. Although a quantity of solutions were proposed to protect the IP of discriminative models, there are very few works targeting generative models.

There are two strategies for IP protection of discriminative DNN models. The first one is *watermarking*. Commonly, a data poisoning based watermarking scheme [42, 1] generates a set of carefully-crafted sample-label pairs as watermarks and embeds them into the protected model during the training process. The labels of the watermark samples should be different from the ground truth to distinguish the protected model from others. The model owner then queries a suspicious black-box model with the watermark samples, and checks the responses for ownership verification. Watermarking solutions suffer from two limitations: (1) they modify the model parameters, which inevitably sacrifices the model performance over normal samples [2]; (2) they were proven to be vulnerable and an adversary can easily remove watermarks from the model [6, 12].

A more promising strategy is *fingerprinting*. Instead of modifying the protected model to give unique behaviors, these approaches [2, 28] craft adversarial examples from the model to precisely characterize its decision boundary. These adversarial examples are carefully designed to exclusively identify the protected model with strong robustness, without impairing model parameters and performance.

In this paper, we focus on the ownership verification of generative models with fingerprinting. It is infeasible to apply the adversarial example based strategy [2, 28] to achieve this goal, due to two reasons. First, adversarial examples and the corresponding inference processes are “anomalous” compared to normal samples. This gives an adversary opportunities to identify verification samples (i.e., adversarial examples) and then manipulate the verification results. Section 4.2 and Figure 4 prove the feasibility of distinguishing verification samples from normal ones by checking the fea-

ture map. Second, adversarial examples for generative models are less robust than discriminative models. Our evaluations in Section 4.4 indicate that common transformations on the protected GAN model and images can easily invalidate the effects of such verification samples, although they exhibit much stronger robustness for discriminative models [2, 28]. One possible reason is that the output of generative models (e.g., images) commonly has larger space than discriminative models (predicted class), and is easier to be changed. This also enables the adversary to break the fingerprinting scheme.

We propose a novel fingerprinting scheme to overcome the above limitations. The key insight of our solution is to *leverage invisible backdoor technique* [20, 22, 38] for *stealthy and robust ownership judgement*. In an invisible backdoor attack, the adversary impairs the victim classifier to give wrong prediction results when the inference samples contain visually invisible triggers, while still functioning correctly for normal samples. Inspired by this, we aim to design the verification samples, whose outputs from the protected model contain invisible triggers to make a backdoor classifier give abnormal results. Meanwhile, their outputs from other unrelated models are still normal for the classifier to make correct predictions. As a result, the model owner can use the backdoor classifier to check the model output and exclusively identify the protected model.

Generating such verification samples and backdoor classifier is challenging. First, we need to make the verification process *stealthy*, where the verification input, model output and feature maps should be indistinguishable from the normal ones. Second, the fingerprint must be *unique* enough to form a strict one-to-one correspondence with the protected model. Third, the fingerprint should be highly *robust* against common model or image transformations possibly enforced by the adversary. More importantly, there exists a trade-off between the uniqueness and robustness properties, which is difficult to balance. To meet these requirements, we devise a novel algorithm to efficiently generate effective verification samples. We also introduce a novel backdoor embedding approach with Unique-Triplet Loss and fine-grained categorization to train the backdoor classifier.

We evaluate our solution with three state-of-the-art models (AttGAN, StarGAN, STGAN) for facial attributes edition. Experiments indicate the fingerprints can distinguish the protected model from others with high confidence. Our fingerprints are unique to the protected model and indistinguishable from clean samples. We also comprehensively validate the robustness of our solution: it is still effective under various model and image transformations.

2. Problem Statement

We focus on Generative Adversarial Networks (GANs), which can synthesize data based on the contest of two neu-

ral networks. Without loss of generality, we consider an image-to-image translation model $G: R^{m \times n} \rightarrow R^{m \times n}$, which maps an input image to an output image. For instance, StarGAN [7] is designed to change the facial attributes of a face, e.g., hair color, nose size, etc. Our scheme can be extended to other types of GANs and tasks as well.

Threat model. We follow the same system setting and assumptions in the discriminative case [2, 28] for our scenario: given a protected generative model G , an adversary may obtain an illegal copy of G and use it for profit without authorization. The goal of the model owner is to detect whether a suspicious model G^s is plagiarized from G . Different from the watermarking mechanisms, we assume the model owner cannot change the original model G , which may compromise the model performance.

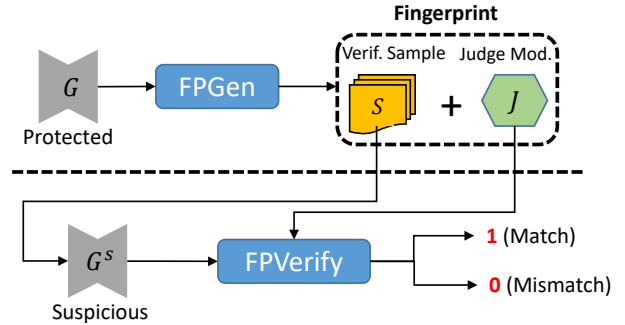


Figure 1: Fingerprint generation and verification.

The model owner has only oracle access to the suspicious model G^s , i.e., he can send arbitrary input to G^s and receive the corresponding output. The adversary may slightly alter the model (e.g., model compression) to make it different from the original one. He can also apply common image transformations over the model output to disrupt the verification results. Such transformations must be performed efficiently and maintain the usability of the model. The model owner needs to have a robust solution for ownership verification against these scenarios.

Fingerprint for GAN. The model owner can adopt DNN *fingerprinting* to protect the IP of his model. The workflow is shown in Figure 1. The owner can generate a fingerprint from his GAN model G , which is a unique identifier for the model to be distinguishable from others. A fingerprint consists of a set of verification sample-label pairs $\mathcal{S} = \{(x_i, y_i)\}_{i=1}^n$ and a judge module \mathcal{J} . During the verification phase, the owner queries the suspicious model G^s with x_i and obtains the corresponding outputs $G^s(x_i)$. He then feeds these outputs to \mathcal{J} , which tells whether the fingerprint matches the model G^s (i.e., G^s is plagiarized from G or not). We formally define a fingerprinting scheme as below:

Definition 1. (*Fingerprint for GAN*) A fingerprinting scheme for GANs is defined as a tuple of probabilistic poly-

nomial time algorithms (**FPGen**, **FPVerify**), where

- **FPGen** generates a fingerprint that consists of verification sample-label pairs $\mathcal{S} = \{(x_i, y_i)\}_{i=1}^n$ and a judge module \mathcal{J} .
- **FPVerify** sends the verification samples to a suspicious generative model G^s and obtains the output images, which are further fed into the judge module \mathcal{J} for fingerprint checking. **FPVerify** outputs 1 if the fingerprint matches the model. Otherwise it outputs 0.

A good fingerprinting scheme should have the following properties, as shown in Figure 2. The first property is uniqueness, where the fingerprint and the generative model need to be in a one-to-one correspondence. In another word, a fingerprint should be able to uniquely identify the corresponding model (①③):

Property 1. (Uniqueness) A fingerprint $(\mathcal{S}, \mathcal{J})$ is said to be unique to the generative model G if the uniqueness index U meets the following condition for $\forall (x, y) \in \mathcal{S}$:

$$U = \Pr(\mathcal{J}(G(x)) = y) - \mathcal{P}^N \geq \epsilon$$

where \mathcal{P}^N represents the probability distribution of verification results for the normal case that a fingerprint does not match the model.

Second, a fingerprint must be robust enough to match the protected model, even the model or the image experiences various transformations (②). This is formulated as below:

Property 2. (Robustness) A fingerprint $(\mathcal{S}, \mathcal{J})$ is said to be robust for the generative model G if the robustness index R meets the following condition for $\forall (x, y) \in \mathcal{S}$:

$$R = \max_T [\Pr(\mathcal{J}((G(x))^T) \neq y)] \leq \epsilon$$

where $(\cdot)^T$ is the output image through possible model transformation or image transformation, which can still maintain the image quality and content.

Third, the verification samples (x) , their outputs $(G(x))$ and the inference behaviors (e.g., feature maps $G_{x,i}$) should be indistinguishable from normal ones (x_0) (④). This is to guarantee that the adversary cannot recognize his model is under verification. Note that this is never considered or achieved in prior works.

Property 3. (Stealthiness) A fingerprint $(\mathcal{S}, \mathcal{J})$ is said to be stealthy for the generative model G if the stealthiness index S meets the following condition for $\forall (x, y) \in \mathcal{S}$:

$$S = \max[\|x, x_0\|, \|G(x), G(x_0)\|, \|G_{x,i}, G_{x_0,i}\|] \leq \epsilon$$

where x_0 is a clean image, $G_{x,i}$ is the i -th feature map in G . and $\|\cdot, \cdot\|$ is a distance function.

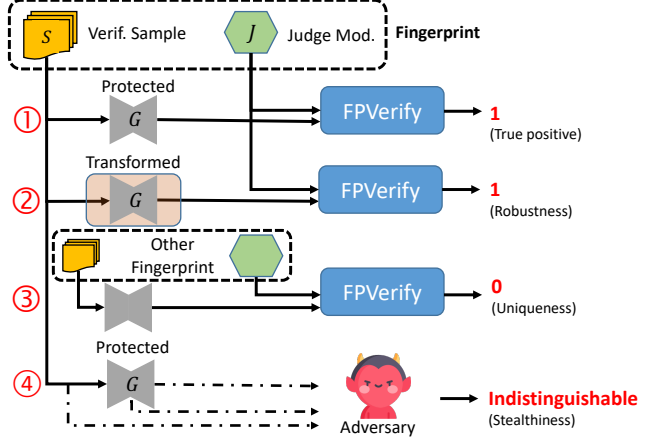


Figure 2: Properties of a good fingerprint.

3. Methodology

We present our novel fingerprinting scheme for generative models, which can achieve the above three properties.

3.1. Insight

As demonstrated in Section 2, a verification sample needs to give similar model output and inference behaviors as a normal sample. However, the judge module is able to recognize the corresponding response of the protected model. The key insight of our solution is that *such verification process is very similar to invisible backdoor attacks* [20, 22, 38], which can guide us to design our expected fingerprints.

In a backdoor attack, an adversary aims to compromise a DNN model such that it maintains correct predictions for normal samples, while giving wrong results for malicious samples which contain a secret trigger [26, 11, 40, 16]. Then researchers proposed invisible backdoor attacks [20, 22, 38], where the trigger is visually invisible, but still able to activate the backdoor in the compromised model to make wrong predictions. Inspired by this technique, we can design the judge module \mathcal{J} as a backdoor classifier, and only the matched model can output an invisible backdoor sample $G(x)$ from the verification sample, which can trigger the classifier to make an unique prediction.

Specifically, we introduce Imperceptible Sensitive (IS) samples as the verification samples in a fingerprint. An IS sample x is constructed from a normal sample x_0 with bounded perturbations. Besides, the corresponding model output $G(x)$ and feature map $G_{x,i}$ are also indistinguishable from those of x_0 . The stealthiness property is thus satisfied during verification. However, this sensitive sample becomes an invisible backdoor sample after being processed by the protected model G , which can mislead a special backdoor classifier f^b to predict

a wrong label y . It is also unique that other unrelated models still output normal samples for f^b to predict correctly. Hence we adopt f^b as the judge module to identify the protected model based on its output of the IS samples.

Generating high-quality IS samples and the corresponding backdoor classifier is more challenging than designing invisible backdoor attacks, since we need to enforce strong uniqueness, robustness as well as stealthiness influenced by the GAN models. Below we introduce novel approaches to construct such samples as well as the backdoor classifier.

3.2. Generating Verification Samples

Our first step is to construct IS samples given the protected model G . These samples should be stealthy, and the model output should be invisible backdoor samples for a backdoor classifier. To achieve this, the owner first prepares a normal classifier f as the judge module, which predicts the attributes of images in the GAN task. Then he adopts the following method to generate the desired samples.

Method. Each IS sample x is crafted from a clean one x_0 . We expect x can maximize the uniqueness index U while minimizing the stealthiness index S . For U , we use $Pr(f(G(x_0)) = y)$ to denote the normal case \mathcal{P}^N that the fingerprint does not match the model. As a result, we have the following objective:

$$\begin{aligned} & \min_x S - U \\ & \approx \min_x \|x - x_0\| + \|G(x) - G(x_0)\| + \sum_i \|G_{x,i} - G_{x_0,i}\| \\ & - L_{CE}(f(G(x)), f(G(x_0))) \end{aligned} \quad (1)$$

where the Cross-Entropy loss $L_{CE}(f(G(x)), f(G(x_0)))$ represents the distance between the two probability distributions $Pr(f(G(x)) = y)$ and $Pr(f(G(x_0)) = y)$.

The above optimization problem can be resolved by conventional optimization-based approaches. Starting from x_0 , we iteratively search for the optimal verification sample x to minimize the above loss function. After x is discovered, we further check if it can satisfy the uniqueness and stealthiness properties defined in Section 2. If so, we can identify a verification sample-label pair (x, y) , where y is an abnormal label different from the ground truth label $y_0 = f(G(x_0))$.

3.3. Training Backdoor Classifier

With Eq.1, the model owner can produce IS samples with good stealthiness and uniqueness. To further improve the verification results, we propose a novel method for the owner to fine-tune the classifier f to be f^b , which has better recognition capability of the verification responses. The objective is formulated as below.

$$\min_T R - U \quad (2)$$

We prepare datasets for fine-tuning the classifier. Let \mathcal{G} be the set of model outputs $G(x)$ for verification samples, and \mathcal{G}_0 be the set of model outputs $G(x_0)$ for the corresponding clean samples. We augment these two sets with common image transformations to generate \mathcal{G}^T and \mathcal{G}_0^T . Then we obtain $\mathcal{G}_b = \mathcal{G} \cup \mathcal{G}^T$ as the set of invisible backdoor samples, and $\mathcal{G}_n = \mathcal{G}_0 \cup \mathcal{G}_0^T$ as the set of normal samples. We propose two techniques to optimize the objective.

Triplet Loss. In an object classification task, pose and illumination can sometimes be more critical to determine the classification results than the object feature itself. Two different objects are more likely to be treated as one type under the same pose and illumination condition. To address this issue, Schroff et al. [31] proposed the Triplet Loss, which can minimize the inner representation (i.e., feature embedding) difference of the same object with different external conditions, while maximizing the difference of different objects with the same condition. This can significantly enhance the classifier’s performance. Similarly, we can leverage the Triplet Loss to fine-tune the backdoor classifier, which can minimize the feature embedding difference between $G(x)$ and $(G(x))^T$ for robustness, and maximize the difference between $G(x)$ and $G(x_0)$ for uniqueness.

Specifically, we use $\mathcal{E}(\cdot)$ to denote the feature embedding of an image, i.e., the classifier f without the classification layers. Then our goal is to optimize the following objective:

$$\min_x \|\mathcal{E}(G(x)), \mathcal{E}((G(x))^T)\| - \|\mathcal{E}(G(x)), \mathcal{E}(G(x_0))\| \quad (3)$$

where x is a verification sample generated from a clean x_0 .

We design a novel Unique-Triplet Loss with a batch-inner mining method to represent the above objective:

$$\begin{aligned} UT = & \sum_{g_a \in B_a} \max\{ \max_{g_p \in B_p} (\|\mathcal{E}(g_a) - \mathcal{E}(g_p)\|) \\ & - \min_{g_n \in B_n} (\|\mathcal{E}(g_a) - \mathcal{E}(g_n)\|) + c, 0 \} \end{aligned} \quad (4)$$

where B_a and B_p are two batches sampled from \mathcal{G}_b , and B_n is a batch sampled from \mathcal{G}_n . Intuitively, for each backdoor sample g_a , we aim to minimize the longest feature embedding distance between g_a and g_p , and maximize the shortest distance between g_a and g_n .

Fine-grained categorization. This computer vision task aims to classify an image into an exact category, e.g., the brand of a car, the species of a bird. Researchers have designed various techniques to achieve this challenging goal [39, 29, 41]. We can treat the backdoor fine-tuning process as a fine-grained categorization task, where samples from \mathcal{G}_b are in one category (matched), while samples from \mathcal{G}_n are in another category (mismatched). Specifically, we change the backdoor classifier to a multi-task one: the original network is used to predict the image attribute, which

is trained using the Cross-Entropy loss L_{CE} ; a new binary classification layer is also added to predict the verification category (matched or mismatched), which is trained using the Entropy-Confusion Loss [9]:

$$EC(y'_b, y_b) = \sum_i \sum_{j=0}^1 \left(y'_{bi,j} \log \frac{y'_{bi,j}}{y_{bi,j}} + y'_{bi,j} \log y'_{bi,j} \right) \quad (5)$$

where y'_b and y_b are the prediction and ground truth of the verification category, respectively.

Our ultimate loss function used to fine-tune the backdoor classifier is

$$\mathcal{L} = L_{CE}(f(g), y) + L_{CE}(f(g_0), y_0) + \lambda * (UT + EC(y'_b, y_b)) \quad (6)$$

Furthermore, the augmented set $\mathcal{G}_b \cup \mathcal{G}_n$ is used to train the backdoor classifier f^b .

3.4. Fingerprint Verification

The model owner uses the generated fingerprint to check whether a suspicious GAN model G^s originates from the protected one G . He first sends each verification sample x to the model G^s , and retrieves the output $G^s(x)$. The verification samples have high stealthiness, so the adversary who controls G^s cannot recognize it is under ownership verification. The owner then feeds $G^s(x)$ to the backdoor classifier f^b . If $f^b(G^s(x))$ is the same as the verification label y , then he has confidence to tell G^s is plagiarized from G .

To increase the verification accuracy, the owner can query G^s with a large quantity of verification samples, and calculate the average accuracy of the predictions with the verification labels. An accuracy above a threshold confirms the piracy of the protected model with high confidence.

4. Experiments

4.1. Configuration and Implementation

Model and dataset. Our scheme is general for various GAN models and tasks. Without loss of generality, we employ three different GANs (e.g. AttGAN [15], StarGAN [7], and STGAN [24]) for evaluations. These models take a face image as input, and produce an image with modified attributes specified by the user. In our experiments, we train each model to edit five attributes: black hair, blond hair, brown hair, male and young. We train and test these models on a public face dataset CelebA [27].

Scheme implementation. We adopt ResNet34 [13] to implement the backdoor classifier f^b . Other state-of-the-art image classification models can be used as well. We train this classifier on the CelebA dataset to predict the facial attributes. Each sample in CelebA has 40 annotated attributes. We set the resolution of the images to $128 * 128$ as the three

Table 1: Top-5 attributes for three GANs in generating the verification samples in GAE.

GAN	Selected fingerprinting attributes
AttGAN	Smiling, BagsUnderEyes, Attractive, MouthSlightlyOpen, HighCheekbones
StarGAN	Smiling, Male, Young, WearingNecklace, Attractive
STGAN	BigNose, Young, Smiling, BagsUnderEyes, HighCheekbones

adopted GANs can achieve the best performance under this setting. We believe our method is effective for other images resolutions as well.

For generating the verification samples, we employ the optimization-based algorithm in Section 3.2 and restrict the distance between $G(x)$ and $G(x_0)$ below 0.0009 under the L_2 -norm. For training the backdoor classifier, we adopt four different image transformations (adding noises, blurring, compression, and cropping) on the model output to augment the datasets. For verification, we randomly select 100 verification samples to query the target model, use f^b to predict the attributes and compare them with the corresponding labels defined in the fingerprint. A match between the label and prediction indicates a fingerprint match.

Baselines. We consider three competitive baselines and compare them with our scheme (IS). The first scheme, called AE, follows the conventional strategy for discriminative models [2, 28]. It generates adversarial examples of the protected GAN model as verification samples. We adopt the C&W technique to generate imperceptible perturbations on the clean samples to keep the model outputs close to the clean samples. For verification, the model owner measures the Euclidean distance between the clean input and output images. A distance smaller than a pre-defined threshold (0.0009 in our experiments) indicates a fingerprint match.

The second baseline, called GAE, crafts verification samples, whose model output images are adversarial examples against an independent facial attribute classifier. This strategy borrows the idea from the works using generative models to produce adversarial patches [36, 23, 32]. Table 1 shows the top-5 facial attributes that will be mispredicted by the classifier for the three GANs. For verification, erroneous predictions for at least 4 of 5 attributes from the classifier indicate fingerprint match. The generated verification samples also satisfy the *stealthiness* property requirement.

The third baseline, called IS-S, follows our design philosophy to generate verification samples, whose model output can trigger a backdoor classifier. We embed the backdoor into the model by simply fine-tuning the model with the loss function

$$L_{CE}(f(g), y) + L_{CE}(f(g_0), y_0),$$

instead of employing our optimization strategies with Unique-Triplet Loss and fine-grained categorization.

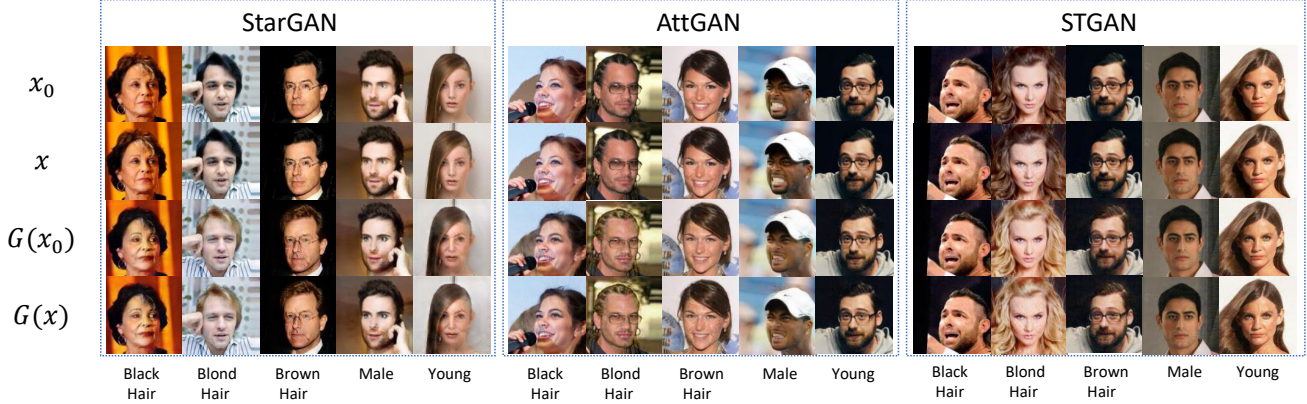


Figure 3: Fingerprint visualization for three GAN models with five edited attributes. (a) Clean sample x_0 ; (b) Verification sample x ; (c) GAN output of clean sample $G(x_0)$; (d) GAN output of verification sample $G(x)$.

Table 2: PSNR and SSIM of the verification and clean input (x , x_0) and output ($G(x)$, $G(x_0)$) images for different edited attributes. A1: Black Hair. A2: Blond Hair. A3: Brown Hair. A4: Male. A5: Young.

Similarity	StarGAN					AttGAN					STGAN				
	A1	A2	A3	A4	A5	A1	A2	A3	A4	A5	A1	A2	A3	A4	A5
PSNR(x , x_0)	41.54	42.38	42.34	41.12	40.86	47.50	45.54	46.41	46.16	46.41	46.22	44.08	43.48	44.56	44.64
SSIM(x , x_0)	0.98	0.98	0.98	0.98	0.98	0.99	0.99	0.99	0.99	0.99	0.99	0.99	0.99	0.99	0.99
PSNR($G(x)$, $G(x_0)$)	37.75	38.00	38.12	37.37	37.20	45.33	43.33	44.38	44.46	44.36	44.53	42.78	42.81	43.94	44.01
SSIM($G(x)$, $G(x_0)$)	0.97	0.97	0.97	0.96	0.96	0.99	0.99	0.99	0.99	0.99	0.99	0.99	0.99	0.99	0.99

Metrics. We expect a good scheme can give abnormal predictions for the matched model, and normal predictions for unrelated models. We adopt Mismatch Score, which is defined as the ratio of verification samples that indicate the model is not matched. Clearly a good fingerprint should have high Mismatch Score for unrelated models, and low Mismatch Score for the matched model. We can use a threshold (0.2 in our experiments) to determine whether a model is matched or not.

4.2. Stealthiness Analysis

Compared to the fingerprinting solutions for discriminative models [2, 28], our method achieves better stealthiness, as demonstrated from the following two aspects.

Visually indistinguishability. In our scheme, the verification samples and the corresponding GAN outputs should look very close to normal samples. Figure 3 visually compares the verification query-response images with the ground-truth (normal images)¹. We observe that the perturbations added to the verification input and output images are imperceptible. So the adversary can hardly notice they are used for fingerprint verification. Table 2 quantitatively shows the peak signal-to-noise ratio (PSNR) and structural similarity (SSIM) between the input of clean and verification images, as well as between their outputs. This can give the same conclusion for the indistinguishability.

¹Visualizations of AE and GAE are in the supplementary materials.

Indistinguishability from the feature map. An adversary may also try to monitor the intermediate results (e.g., feature map) to detect the abnormal verification samples. Prior works leveraged such strategy to detect adversarial examples [34, 17, 19]. To evaluate this detection possibility, we follow the method in [19] to compute the distributions of standard deviations of feature maps for inference of 100 normal and 100 verification samples, respectively. Figure 4 compares the distributions of these different fingerprinting schemes. The Kolmogorov-Smirnov statistic [3] for each case is 0.69, 0.41 and 0.29, respectively. We observe a significant difference between these two distributions for adversarial example-based schemes (AE and GAE). In contrast, the distributions are very close for our scheme (IS), so it is hard for the adversary to differentiate normal and verification samples.

Before analyzing the robustness and the uniqueness of these methods, we need to point that there is a trade-off between the robustness and the uniqueness. If we want a higher uniqueness, the verification will be more strict. If we want a higher robustness, the verification will be more tolerant.

4.3. Uniqueness Analysis

A good fingerprinting scheme should be *unique*: the fingerprint (verification samples and backdoor classifier) should exclusively match the GAN model it is generated

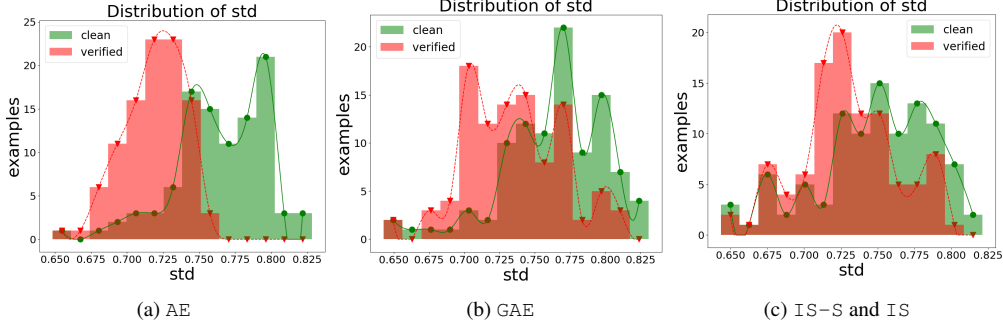


Figure 4: Feature map distributions for normal (green) and verification (red) samples.

Table 3: Mismatch Score for verifying different models. \downarrow means a lower score is better. \uparrow means a higher score is better. Same for the following tables.

GAN Structure	Method	Original (\downarrow)	Other GAN (\uparrow)		
			StarGAN	AttGAN	STGAN
StarGAN	AE	0.00	100.00	100.00	100.00
	GAE	0.00	49.80	66.20	69.60
	IS-S	5.88	37.90	84.90	73.00
	IS	9.30	72.85	82.15	69.90
AttGAN	AE	0.00	100.00	100.00	100.00
	GAE	0.00	71.00	57.80	60.20
	IS-S	7.55	50.90	65.80	42.98
	IS	9.95	60.38	87.47	83.08
STGAN	AE	0.00	100.00	100.00	87.00
	GAE	0.00	73.80	74.20	32.20
	IS-S	8.43	49.48	57.92	16.80
	IS	9.82	69.95	71.25	30.95

from. We evaluate this property from two perspectives.

Model uniqueness. We generate verification samples from one GAN model, and use them to verify the model itself, as well as other unrelated GAN models, including a model retrained with the same algorithm and network structure. Table 3 shows the Mismatch Scores for different models. We observe all the four methods can correctly identify the matched model (low score values in the “Original” column). For unrelated models, AE gives the best results with very high Mismatch Score. In contrast, IS-S performs worse, especially for differentiating the unrelated STGAN from the protected STGAN (16.8%). Our scheme significantly outperforms IS-S due to the adoption of advanced backdoor embedding techniques.

Judge module uniqueness. We also need the judge module (i.e., backdoor classifier) to be special, and other classifiers do not work for verification. We train different types of attribute classifiers with the same or different network structures, and replace the original one to predict the output of verification samples for the matched GAN model. Table 4 summarizes the results². We observe these methods exhibit great uniqueness for the judge module: other classifiers cannot be used for verification. IS-S and IS are more effective as the Mismatch Scores are very high. This

Table 4: Mismatch Score using different classifiers.

GAN Structure	Method	Original (\downarrow)	Other Classifier (\uparrow)		
			ResNet34	MobileNetv2	VGG19
StarGAN	GAE	0.00	38.00	45.80	46.80
	IS-S	5.88	90.08	90.93	91.15
	IS	9.95	90.08	90.93	91.15
AttGAN	GAE	0.00	41.00	48.60	48.60
	IS-S	7.55	90.28	90.93	90.95
	IS	9.30	90.28	90.93	90.95
STGAN	GAE	0.00	67.20	70.40	73.00
	IS-S	8.43	89.33	90.78	90.25
	IS	9.82	89.33	90.78	90.25

is because the other classifiers do not contain the backdoor and cannot recognize the invisible backdoor samples of the model output.

4.4. Robustness Analysis

Robustness requires the fingerprint should still remain effective when the suspicious model or the verification samples are transformed by the adversary. We perform our evaluations in these two directions.

Robustness against model transformation. We consider two types of model transformation methods: model fine-tuning with different number of epochs, and parameter pruning with different compression ratios. Table 5 reports the Mismatch Scores for the three matched GAN models. We can observe that AE is not robust against model pruning with very high Mismatch Scores. It is neither robust against model fine-tuning, especially for StarGAN. In contrast, our method and the other two baselines achieve stronger robustness under these model transformations.

Robustness against image transformation. The adversary may adopt image transformations to process the model output, making it hard to be recognized by the classifier. We consider four common transformations: *adding Gaussian noises* (with mean $\mu = 0$ and standard deviation $\sigma = 0.1$), *blurring* (with a kernel size of 5), *JPEG compression* (with a compression ratio of 35%), and *cropping* (from 128*128 into 100*100). Table 6 reports the verification results³.

²We do not consider AE since it does not need a classifier.

³We also consider the impacts of different transformation strengths on

Table 5: Mismatch Score after model transformations (Fine-tuning and Pruning) with different settings.

GAN Structure	Method	Original (\downarrow)	Fine-tuning (\downarrow)			Pruning (\downarrow)	
			10	20	30	0.2	0.4
StarGAN	AE	0.00	100.00	94.00	98.00	57.00	100.00
	GAE	0.00	5.80	8.20	4.00	1.80	3.00
	IS-S	5.88	6.93	10.75	7.85	5.88	6.40
	IS	9.95	14.68	15.43	15.20	9.88	10.43
AttGAN	AE	0.00	9.00	16.00	25.00	78.00	100.00
	GAE	0.00	5.40	4.60	5.20	2.80	12.60
	IS-S	7.55	7.63	7.60	7.63	7.60	11.00
	IS	9.30	9.38	9.30	9.33	9.25	15.05
STGAN	AE	0.00	15.00	25.00	27.00	42.00	100.00
	GAE	0.00	4.60	4.80	5.40	5.00	13.40
	IS-S	8.43	8.38	8.28	8.20	8.55	8.60
	IS	9.82	9.70	9.75	9.60	9.78	16.65

Table 6: Mismatch Score after four image transformations.

GAN Structure	Method	Original (\downarrow)	Image Transformation (\downarrow)			
			Noise	Blur	JPEG	Crop
StarGAN	AE	0.00	99.00	100.00	100.00	100.00
	GAE	0.00	22.40	15.40	11.00	18.40
	IS-S	5.88	6.88	6.43	6.25	6.43
	IS	9.95	13.98	12.43	10.30	9.38
AttGAN	AE	0.00	99.00	100.00	100.00	100.00
	GAE	0.00	18.00	27.00	15.20	23.20
	IS-S	7.55	8.80	7.93	7.48	8.43
	IS	9.30	19.68	15.90	10.70	11.18
STGAN	AE	0.00	100.00	100.00	100.00	100.00
	GAE	0.00	23.00	58.80	34.80	43.00
	IS-S	8.43	11.00	9.28	8.55	9.05
	IS	9.82	13.60	13.45	11.85	11.20

Similarly, we observe AE is not robust at all. These transformations can significantly distort the model output. GAE is less effective for STGAN models. In contrast, the backdoor-based approaches perform the best as the backdoor classifiers and invisible backdoor samples are more robust against these operations.

4.5. Summary

From the above evaluations, we can see the adversarial example-based solutions (AE and GAE) are not stealthy, especially from the feature space. This also confirms with the prior methodologies for detecting adversarial examples. AE is unique for the fingerprinted models, but not robust enough against model pruning, fine-tuning or image transformations. GAE does not show high uniqueness for different classifiers or robustness against image transformations. Uniqueness and robustness are equally important for a fingerprinting scheme because others can use many image transformations to avoid the model being detected. When we compare Table 3 and Table 5 together, we can find that, although the AE has very high uniqueness, it totally fails in robustness test. While our IS does not have the highest uniqueness and robustness, it keeps the best balance between the uniqueness and robustness.

In contrast, the backdoor-based solutions (IS-S and IS) show better results for meeting those properties. Particularly, IS is better than IS-S for the uniqueness of distinguishing matched and unmatched models, due to the adop-

tion of Triplet Loss and fine-grained categorization.

tion of Triplet Loss and fine-grained categorization.

5. Related Works

Watermarking DNN Models. This strategy is to embed watermarks into the DNN models for ownership verification. Existing watermarking schemes can be classified into two categories: (1) parameter-embedding solutions [33, 30, 4] inject watermarks into the model parameters while preserving the model’s performance. For example, [33] embedded a bit-vector (signature) into the model parameters via a carefully-designed parameter regularizer. (2) Data-poisoning solutions take a set of unique sample-label pairs as watermarks and embed their correlation into discriminative models during the training process. To preserve the fidelity and robustness of the watermarked models, the essential part of data-poisoning watermarking schemes is the generation of watermark samples. For examples, [42, 1] leveraged the DNN backdoor attacks to embed backdoor samples with certain trigger patterns into discriminative models; [18, 21] adopts imperceptible perturbations as the verification samples. Chen et al. [5] designed temporal state sequences to watermark reinforcement learning models. Lou et al. [37] leverages cache side channels to verify watermarks embedded in the model architecture.

However, these watermarking schemes were empirically proven to be vulnerable to watermark removal attacks [6, 12]. Besides, embedding watermarks into the model requires the changes of model parameters, and can compromise the model performance to some extent [2]. These limitations can be addressed by DNN model fingerprinting, as adopted in this paper.

Fingerprinting DNN Models. A few works have proposed fingerprinting schemes for discriminative models. These solutions leveraged adversarial examples as fingerprints to identify the target discriminative models. For example, IPGuard [2] identified the data samples close to the target model’s classification boundary to fingerprint this model. [28] adopted conferrable adversarial examples with certain labels, which can transfer from the target model to its surrogates, while remaining ineffective to other models. A prior work [14] designed sensitive samples to fingerprint black-box models, which will fail even the model has very small modifications.

Due to the fundamental differences between discriminative and generative models, these methods can not be easily extended to the protection of GAN models. Besides, existing fingerprints show abnormal behaviors on the model output and feature maps, which give opportunities for the adversary to discover the verification process and then manipulate the results. In this paper, we are the first to focus on fingerprinting the more complicated generative models. Our solution significantly extend the IP protection scenarios and can achieve much stronger stealthiness and robustness

under various scenarios than prior works.

6. Conclusion

In this paper, we introduce a novel fingerprinting scheme to protect the Intellectual Property of generative models. We design a new optimization-based algorithm for the owner to generate verification samples, which leads the target GAN model to fabricate invisible backdoor samples for a backdoor classifier. We propose a novel approach to efficiently embed backdoor into the classifier using Unique-Triplet Loss and fine-grained categorization. Experiments validate that our method can generate effective and stealthy fingerprints for image-to-image translation GAN models. The fingerprints are also robust against various model and image transformations. In the future, we will explore more optimization-based strategies to improve the robustness and effectiveness of our solution, and apply it to different types of GAN models.

References

- [1] Yossi Adi, Carsten Baum, Moustapha Cisse, Benny Pinkas, and Joseph Keshet. Turning your weakness into a strength: Watermarking deep neural networks by backdooring. In *Proc. of the USENIX*, pages 1615–1631, 2018. 1, 8
- [2] Xiaoyu Cao, Jinyuan Jia, and Neil Zhenqiang Gong. IPGuard: Protecting the intellectual property of deep neural networks via fingerprinting the classification boundary. *CoRR*, abs/1910.12903, 2019. 1, 2, 5, 6, 8
- [3] Indra M Chakravarty, JD Roy, and Radha Govind Laha. Handbook of methods of applied statistics. 1967. 6
- [4] Huili Chen, Bitu Darvish Rohani, and Farinaz Koushanfar. DeepMarks: A digital fingerprinting framework for deep neural networks. *CoRR*, abs/1804.03648, 2018. 8
- [5] Kangjie Chen, Shangwei Guo, Tianwei Zhang, Shuxin Li, and Yang Liu. Temporal watermarks for deep reinforcement learning models. In *Proc. of the AAMAS*, 2021. 8
- [6] Xinyun Chen, Wenxiao Wang, Chris Bender, Yiming Ding, Ruoxi Jia, Bo Li, and Dawn Song. REFIT: A unified watermark removal framework for deep learning systems with limited data. *CoRR*, abs/1911.07205, 2019. 1, 8
- [7] Yunje Choi, Minje Choi, Munyoung Kim, Jung-Woo Ha, Sunghun Kim, and Jaegul Choo. StarGAN: Unified generative adversarial networks for multi-domain image-to-image translation. In *Proc. of the CVPR*, pages 8789–8797, 2018. 2, 5
- [8] Ugur Demir and Gozde Unal. Patch-based image inpainting with generative adversarial networks. *CoRR*, abs/1803.07422, 2018. 1
- [9] Abhimanyu Dubey, Otkrist Gupta, Ramesh Raskar, and Nikhil Naik. Maximum-Entropy Fine Grained Classification. In Samy Bengio, Hanna M. Wallach, Hugo Larochelle, Kristen Grauman, Nicolò Cesa-Bianchi, and Roman Garnett, editors, *Proc. of the NeurIPS*, pages 635–645, 2018. 5
- [10] Ian J. Goodfellow, Jean Pouget-Abadie, Mehdi Mirza, Bing Xu, David Warde-Farley, Sherjil Ozair, Aaron C. Courville, and Yoshua Bengio. Generative Adversarial Nets. In Zoubin Ghahramani, Max Welling, Corinna Cortes, Neil D. Lawrence, and Kilian Q. Weinberger, editors, *Proc. of the NeurIPS*, pages 2672–2680, 2014. 1
- [11] Tianyu Gu, Brendan Dolan-Gavitt, and Siddharth Garg. Badnets: Identifying vulnerabilities in the machine learning model supply chain. *CoRR*, abs/1708.06733, 2017. 3
- [12] Shangwei Guo, Tianwei Zhang, Han Qiu, Yi Zeng, Tao Xiang, and Yang Liu. The hidden vulnerability of watermarking for deep neural networks. *CoRR*, abs/2009.08697, 2020. 1, 8
- [13] Kaiming He, Xiangyu Zhang, Shaoqing Ren, and Jian Sun. Deep residual learning for image recognition. In *Proc. of the CVPR*, pages 770–778, 2016. 5
- [14] Zecheng He, Tianwei Zhang, and Ruby Lee. Sensitive-sample fingerprinting of deep neural networks. In *Proc. of the CVPR*, pages 4729–4737, 2019. 8
- [15] Zhenliang He, Wangmeng Zuo, Meina Kan, Shiguang Shan, and Xilin Chen. AttGAN: Facial attribute editing by only changing what you want. *IEEE Transactions on Image Processing*, 28(11):5464–5478, 2019. 1, 5
- [16] Kaidi Jin, Tianwei Zhang, Chao Shen, Yufei Chen, Ming Fan, Chenhao Lin, and Ting Liu. A unified framework for analyzing and detecting malicious examples of DNN models. *CoRR*, abs/2006.14871, 2020. 3
- [17] Ziv Katzir and Yuval Elovici. Detecting adversarial perturbations through spatial behavior in activation spaces. In *Proc. of the IJCNN*, pages 1–9, 2019. 6
- [18] Erwan Le Merrer, Patrick Perez, and Gilles Trédan. Adversarial frontier stitching for remote neural network watermarking. *Neural Computing and Applications*, pages 1–12, 2019. 8
- [19] Kimin Lee, Kibok Lee, Honglak Lee, and Jinwoo Shin. A Simple Unified Framework for Detecting Out-of-Distribution Samples and Adversarial Attacks. In Samy Bengio, Hanna M. Wallach, Hugo Larochelle, Kristen Grauman, Nicolò Cesa-Bianchi, and Roman

- Garnett, editors, *Proc. of the NeurIPS*, pages 7167–7177, 2018. 6
- [20] Shaofeng Li, Benjamin Zi Hao Zhao, Jiahao Yu, Minhui Xue, Dali Kaafar, and Haojin Zhu. Invisible backdoor attacks against deep neural networks. *CoRR*, abs/1909.02742, 2019. 2, 3
- [21] Zheng Li, Chengyu Hu, Yang Zhang, and Shanqing Guo. How to prove your model belongs to you: A blind-watermark based framework to protect intellectual property of DNN. In *Proc. of the ACSAC*, pages 126–137, 2019. 8
- [22] Cong Liao, Haoti Zhong, Anna Squicciarini, Sencun Zhu, and David Miller. Backdoor embedding in convolutional neural network models via invisible perturbation. In *Proc. of the CODASPY*, pages 97–108, 2020. 2, 3
- [23] Aishan Liu, Xianglong Liu, Jiabin Fan, Yuqing Ma, Anlan Zhang, Huiyuan Xie, and Dacheng Tao. Perceptual-sensitive gan for generating adversarial patches. In *Proc. of the AAAI*, pages 1028–1035, 2019. 5
- [24] Ming Liu, Yukang Ding, Min Xia, Xiao Liu, Errui Ding, Wangmeng Zuo, and Shilei Wen. STGAN: A unified selective transfer network for arbitrary image attribute editing. In *Proc. of the CVPR*, pages 3673–3682, 2019. 5
- [25] Ming-Yu Liu, Thomas Breuel, and Jan Kautz. Unsupervised image-to-image translation networks. *Neural Networks*, 131:50–63, 2020. 1
- [26] Yingqi Liu, Shiqing Ma, Yousra Aafer, Wen-Chuan Lee, Juan Zhai, Weihang Wang, and Xiangyu Zhang. Trojaning attack on neural networks. *Security and Communication Networks*, 2019:1–12, 2019. 3
- [27] Ziwei Liu, Ping Luo, Xiaogang Wang, and Xiaoou Tang. Deep learning face attributes in the wild. In *Proc. of the ICCV*, pages 3730–3738, 2015. 5
- [28] Nils Lukas, Yuxuan Zhang, and Florian Kerschbaum. Deep neural network fingerprinting by conferrable adversarial examples. *CoRR*, abs/1912.00888, 2019. 1, 2, 5, 6, 8
- [29] Wei Luo, Xitong Yang, Xianjie Mo, Yuheng Lu, Larry Davis, Jun Li, Jian Yang, and Ser-Nam Lim. Cross-X Learning for Fine-Grained Visual Categorization. In *Proc. of the ICCV*, pages 8241–8250, 2019. 4
- [30] Bitan Darvish Rouhani, Huili Chen, and Farinaz Koushanfar. Deepsigns: An end-to-end watermarking framework for protecting the ownership of deep neural networks. In *Proc. of the ASPLOS*, 2019. 8
- [31] Florian Schroff, Dmitry Kalenichenko, and James Philbin. FaceNet: A unified embedding for face recognition and clustering. In *Proc. of the CVPR*, pages 815–823, 2015. 4
- [32] Yang Song, Rui Shu, Nate Kushman, and Stefano Ermon. Constructing unrestricted adversarial examples with generative models. In *Proc. of the NeurIPS*, pages 8322–8333, 2018. 5
- [33] Yusuke Uchida, Yuki Nagai, Shigeyuki Sakazawa, and Shin’ichi Satoh. Embedding watermarks into deep neural networks. In *Proc. of the ICMR*, pages 269–277, 2017. 8
- [34] Jingyi Wang, Guoliang Dong, Jun Sun, Xinyu Wang, and Peixin Zhang. Adversarial sample detection for deep neural network through model mutation testing. In *Proc. of the ICSE*, pages 1245–1256, 2019. 6
- [35] Ting-Chun Wang, Ming-Yu Liu, Jun-Yan Zhu, Andrew Tao, Jan Kautz, and Bryan Catanzaro. High-resolution image synthesis and semantic manipulation with conditional gans. In *Proc. of the CVPR*, pages 8798–8807, 2018. 1
- [36] Chaowei Xiao, Bo Li, Jun-Yan Zhu, Warren He, Mingyan Liu, and Dawn Song. Generating adversarial examples with adversarial networks. In *Proc. of the IJCAI*, pages 3905–3911, 2018. 5
- [37] Lou Xiaoxuan, Guo Shangwei, Zhang Tianwei, Liu Yang, et al. When nas meets watermarking: Ownership verification of dnn models via cache side channels. *CoRR*, abs/2102.03523, 2021. 8
- [38] Mingfu Xue, Can He, Jian Wang, and Weiqiang Liu. Backdoors hidden in facial features: a novel invisible backdoor attack against face recognition systems. *Peer-to-Peer Networking and Applications*, pages 1–17, 2021. 2, 3
- [39] Ze Yang, Tiange Luo, Dong Wang, Zhiqiang Hu, Jun Gao, and Liwei Wang. Learning to Navigate for Fine-Grained Classification. In *Proc. of the ECCV*, volume 11218, pages 438–454, 2018. 4
- [40] Yi Zeng, Han Qiu, Shangwei Guo, Tianwei Zhang, Meikang Qiu, and Bhavani Thuraisingham. Deep-sweep: An evaluation framework for mitigating dnn backdoor attacks using data augmentation. In *Proc. of the AsiaCCS*, 2021. 3
- [41] Fan Zhang, Meng Li, Guisheng Zhai, and Yizhao Liu. Multi-branch and Multi-scale Attention Learning for Fine-Grained Visual Categorization. In Jakub Lokoc, Tomás Skopal, Klaus Schoeffmann, Vasileios Mezaris, Xirong Li, Stefanos Vrochidis, and Ioannis Patras, editors, *Proc. of the MMM*, pages 136–147, 2021. 4
- [42] Jialong Zhang, Zhongshu Gu, Jiyong Jang, Hui Wu, Marc Ph Stoecklin, Heqing Huang, and Ian Molloy. Protecting intellectual property of deep neural networks with watermarking. In *Proc. of the AsiaCCS*, pages 159–172, 2018. 1, 8

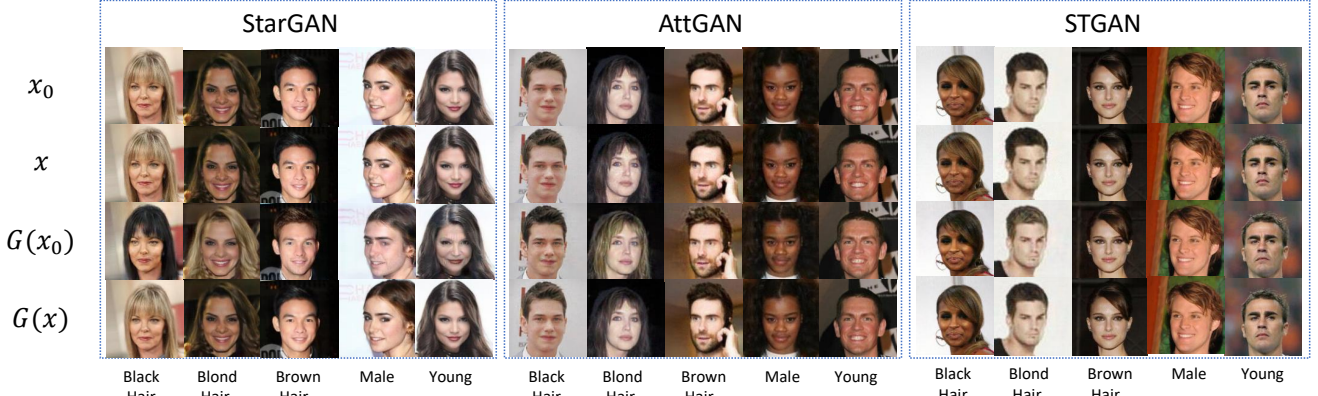


Figure 5: Fingerprint visualization generated from AE for three GAN models with five edited attributes. (a) Clean sample x_0 ; (b) Verification sample x ; (c) GAN output of clean sample $G(x_0)$; (d) GAN output of verification sample $G(x)$.



Figure 6: Fingerprint generated from GAE visualization for three GAN models with five edited attributes. (a) Clean sample x_0 ; (b) Verification sample x ; (c) GAN output of clean sample $G(x_0)$; (d) GAN output of verification sample $G(x)$.

A. Verification Samples of AE and GAE

In this section, we show the verification samples of AE and GAE in Figure 5 and 6, respectively. Additionally, we also present the visualization of our IS in Figure 7 for better presentation to our readers. Table 7 shows the PSNR and SSIM of AE, GAE, and our IS for presenting the quality of verification samples quantitatively. We can find that our IS has higher stealthiness than AE and GAE.

B. High-resolution Facial Images of IS

In our experiments, we evaluate the performance of our proposed method by verifying whether the generated fingerprints satisfy the *uniqueness*, *robustness*, and *stealthiness* properties. Here, we present the high-resolution of GAN output in suffering various degradations, including additive noises, model compression, and corruptions with common image transformations.

B.1. Verification Samples after Different GANs

In Figure 8, we show our verification samples' outputs for different GANs. The columns from (e) to (j) indicate the output images from different models manipulated on both clean samples and verification samples.

B.2. Verification Samples suffer Degradation

In evaluating the robustness of our proposed method, we mainly consider the two different degradation, model compression and common image transformations.

Model Compression. In evaluating the robustness against model compression, we explore the effectiveness of our method when the GAN model is compressed in various levels. In Figure 9, the column (e) to (h) indicate the manipulated images with compressed models when the pruning rate is not larger than 0.4. We can find that the GAN outputs maintain a high-quality visualization, thus the pruning

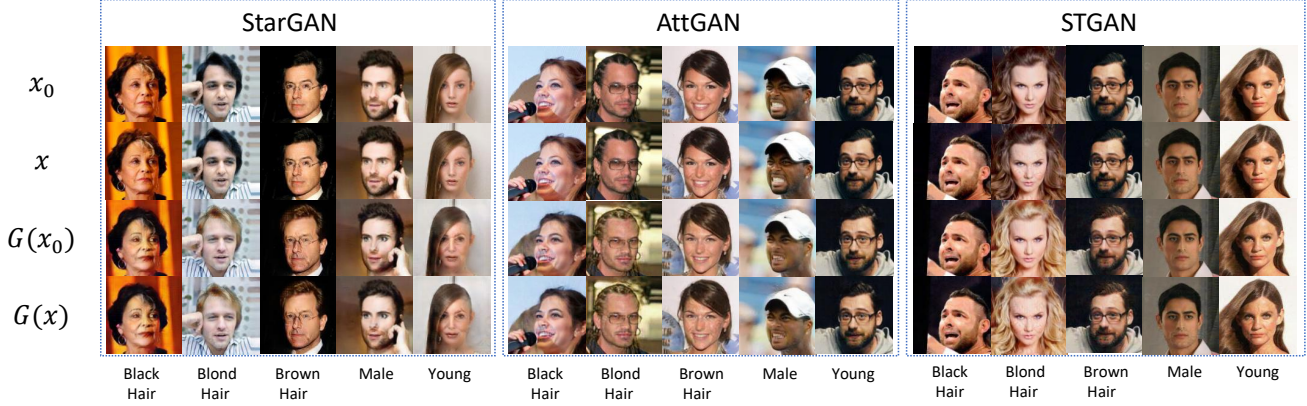


Figure 7: Fingerprint visualization IS for three GAN models with five edited attributes. (a) Clean sample x_0 ; (b) Verification sample x ; (c) GAN output of clean sample $G(x_0)$; (d) GAN output of verification sample $G(x)$.

Table 7: PSNR and SSIM of the verification and clean input (x , x_0) and output ($G(x)$, $G(x_0)$) images for different edited attributes. A1: Black Hair. A2: Blond Hair. A3: Brown Hair. A4: Male. A5: Young.

Similarity		StarGAN					AttGAN					STGAN				
		A1	A2	A3	A4	A5	A1	A2	A3	A4	A5	A1	A2	A3	A4	A5
PSNR(x, x_0)	AE	43.84	43.73	43.64	43.72	43.99	39.92	38.68	38.65	39.60	40.07	38.27	38.23	39.50	39.73	39.36
	GAE	41.32	41.44	41.19	41.44	41.48	42.46	42.60	41.95	43.45	42.64	42.59	42.76	42.52	41.93	41.93
	IS	41.54	42.38	42.34	41.12	40.86	47.50	45.54	46.41	46.16	46.41	46.22	44.08	43.48	44.56	44.64
SSIM(x, x_0)	AE	0.99	0.99	0.99	0.99	0.99	0.96	0.95	0.95	0.96	0.96	0.97	0.97	0.98	0.97	0.98
	GAE	0.98	0.98	0.98	0.98	0.98	0.98	0.98	0.98	0.99	0.98	0.98	0.98	0.98	0.98	0.98
	IS	0.98	0.98	0.98	0.98	0.98	0.99	0.99	0.99	0.99	0.99	0.99	0.99	0.99	0.99	0.99
PSNR($G(x), G(x_0)$)	AE	22.44	18.28	23.37	24.59	23.98	30.83	27.79	29.04	29.43	29.66	31.78	33.82	36.32	37.29	36.87
	GAE	36.94	37.27	37.10	37.30	37.59	41.12	40.74	40.11	41.71	40.76	41.68	41.89	41.64	41.26	41.00
	IS	37.75	38.00	38.12	37.37	37.20	45.33	43.33	44.38	44.46	44.36	44.53	42.78	42.81	43.94	44.01
SSIM($G(x), G(x_0)$)	AE	0.84	0.79	0.87	0.87	0.85	0.95	0.92	0.92	0.94	0.94	0.96	0.97	0.98	0.98	0.98
	GAE	0.95	0.96	0.96	0.96	0.96	0.98	0.98	0.98	0.98	0.98	0.98	0.98	0.98	0.98	0.98
	IS	0.97	0.97	0.97	0.96	0.96	0.99	0.99	0.99	0.99	0.99	0.99	0.99	0.99	0.99	0.99

rate no more than 0.4 is an appropriate setting in our experiment. More experimental results show in the Figure 10.

Image Transformations. The GAN outputs will always be corrupted by various image transformations when spreading in the social networks. Figure 11 presents the visualization of GAN output by employing four different types of common image transformations, including adding *Gaussian noises*, *blurring*, *JPEG compression*, and *centering cropping*. Here, the parameters of these transformations are described in Section 4.4.

In Figure 12, we show the Mismatch Score under different transformation magnitudes, which transformation applies on the output of the GAN. Furthermore, in Figure 13, 14 and 15, we show the Mismatch Score under different transformation magnitudes of AE, GAE, IS-S and IS, in which transformation applies on the input of the GAN. The Mismatch Score in these figures is significantly high. It is because when we add image transformations on the inputs, the outputs of the GAN have more distortions, especially under blurring and compression, which introduce stronger noise to replace our backdoor perturbation. However, when we apply very strong image transformations on the inputs,

the outputs of GAN are in a low quality. We think that strong image transformations will not be used in practice.

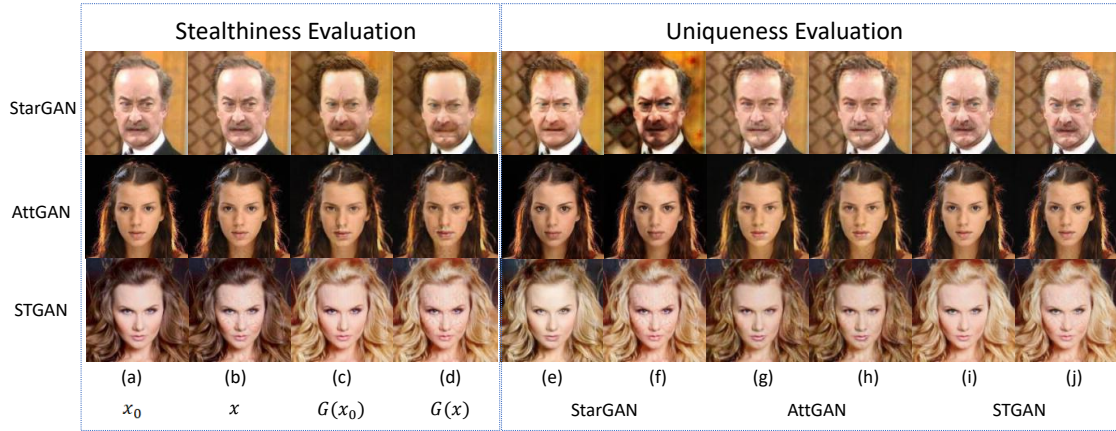


Figure 8: Manipulated images from StarGAN, AttGAN, and STGAN. The column (e) edits attribute on x_0 with StarGAN, the column (f) edits attribute on x with StarGAN, the column (g) edits attribute on x_0 with AttGAN, the column (h) edits attribute on x with AttGAN, the column (i) edits attribute on x_0 with STGAN, the column (j) edits attribute on x with STGAN.

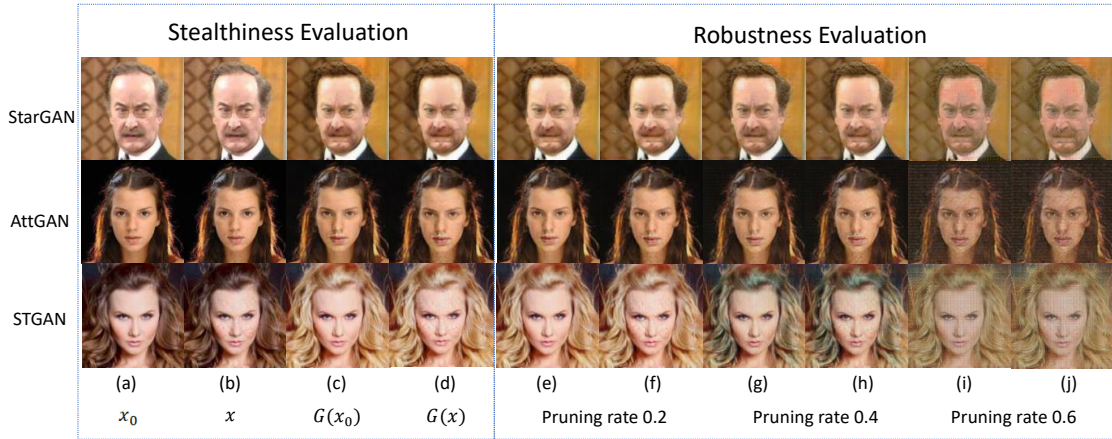


Figure 9: Images manipulated by StarGAN, AttGAN and STGAN. The column (e) edits attributes on x_0 with pruning rate 0.2, the column (f) edits attributes on x with pruning rate 0.2, the column (g) edits attributes on x_0 with pruning rate 0.4, the column (h) edits attributes on x with pruning rate 0.4, the column (i) edits attributes on x_0 with pruning rate 0.6, the column (j) edits attributes on x with pruning rate 0.6.

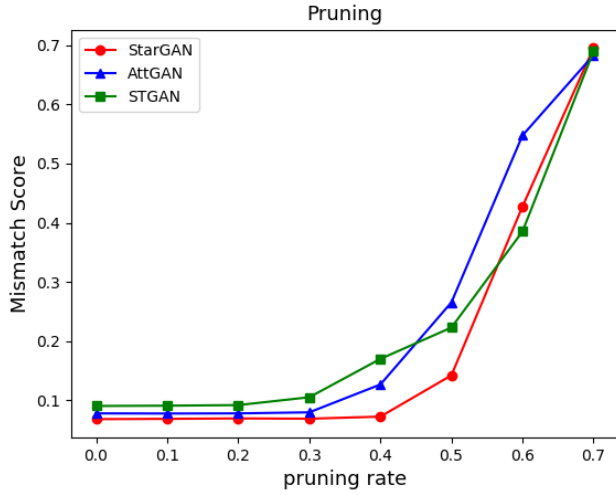


Figure 10: Mismatch Score of IS under different pruning rates.

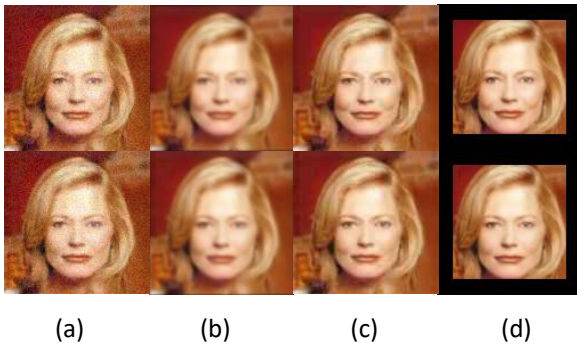


Figure 11: Visualization of GAN output images corrupted by four types of image transformations. The first row and third row are GAN outputs from clean images. The second row and fourth row are GAN outputs from verification samples. (a) adding Gaussian Noise, (b) blurring, (c) JPEG compression, (d) centering cropping.

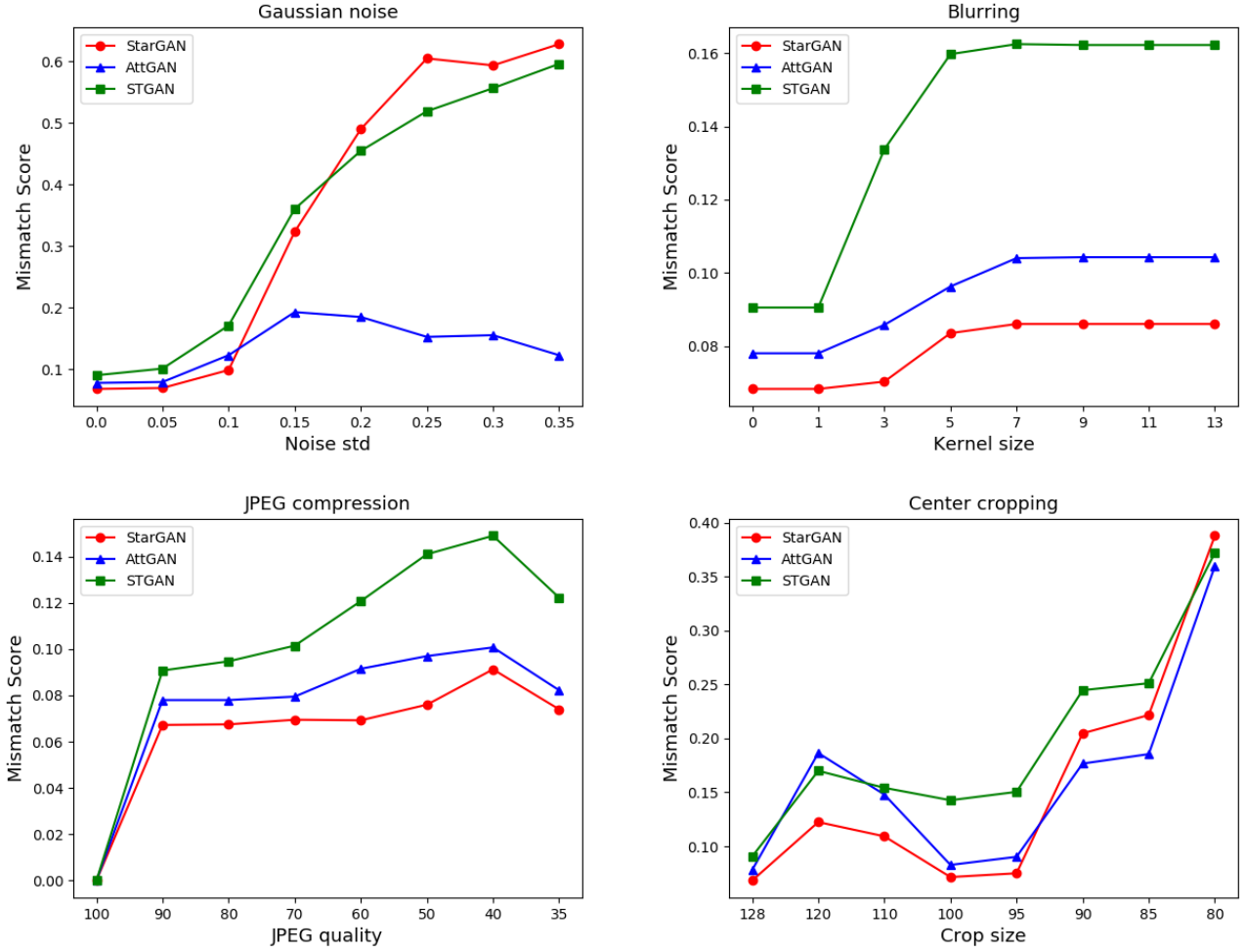


Figure 12: Mismatch Score of IS under different settings of transformations, which are applied on the outputs of the GAN.

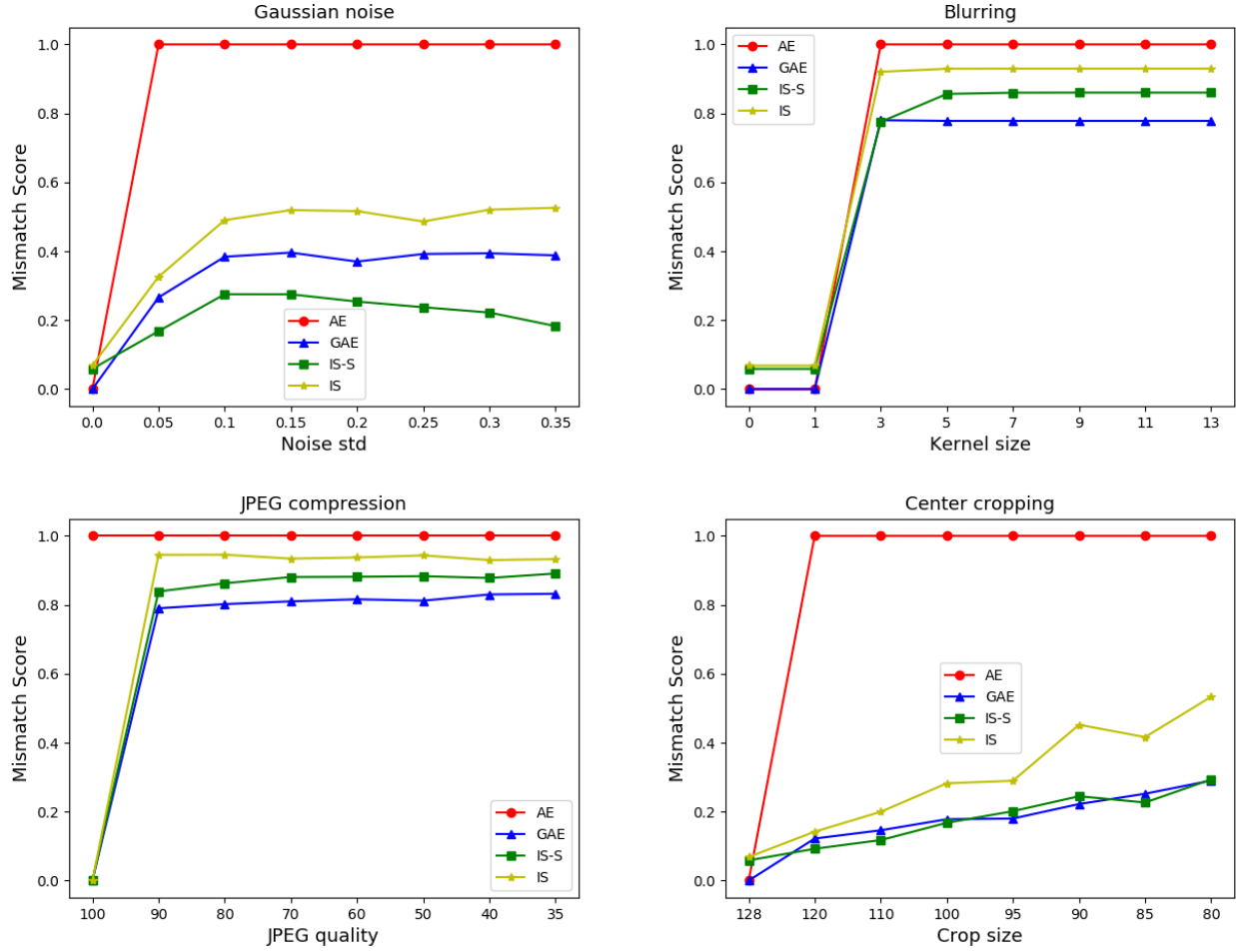


Figure 13: Mismatch Score of StarGAN under different settings of transformations, which are applied on the inputs of the GAN.

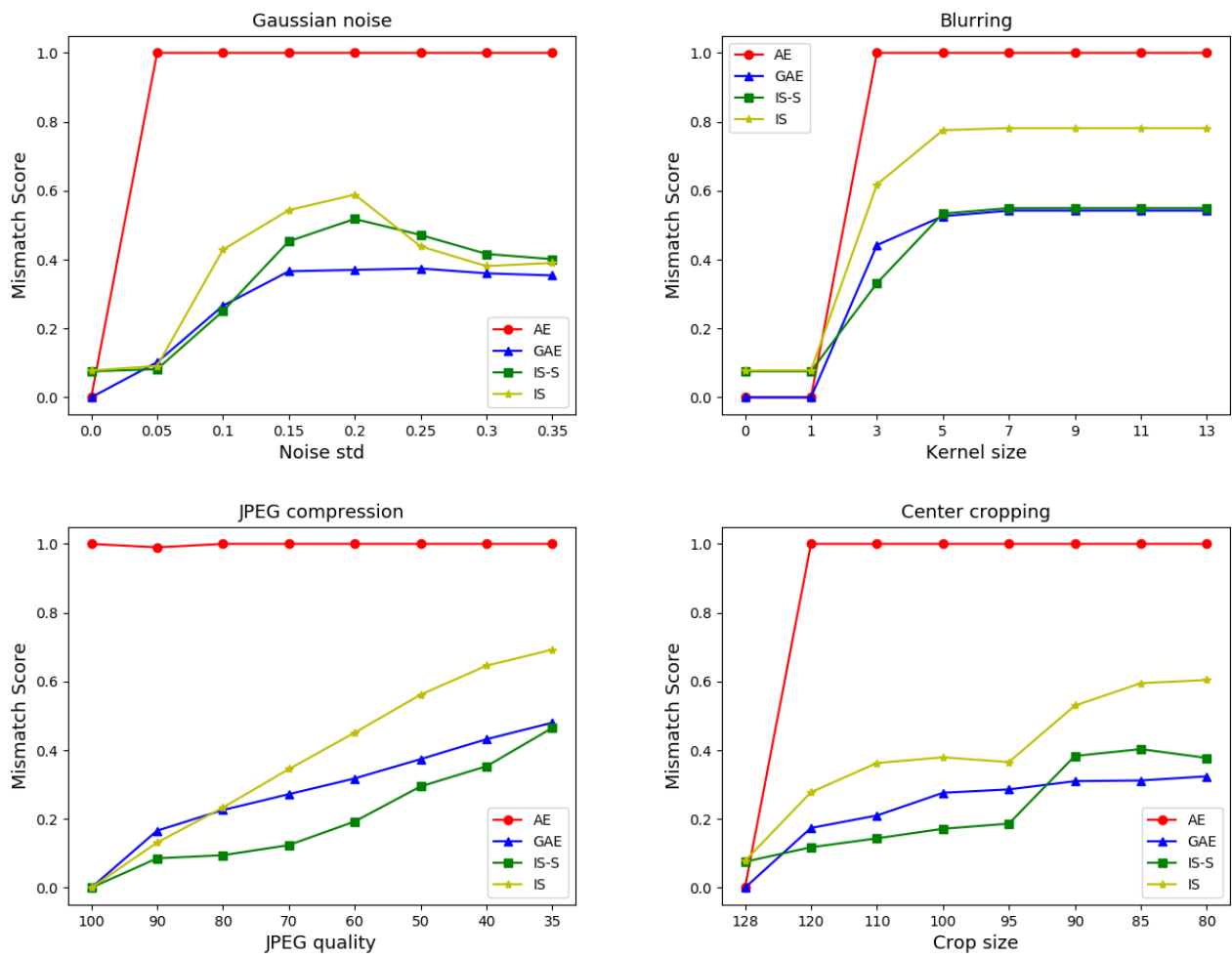


Figure 14: Mismatch Score of AttGAN under different settings of transformations, which are applied on the inputs of the GAN.

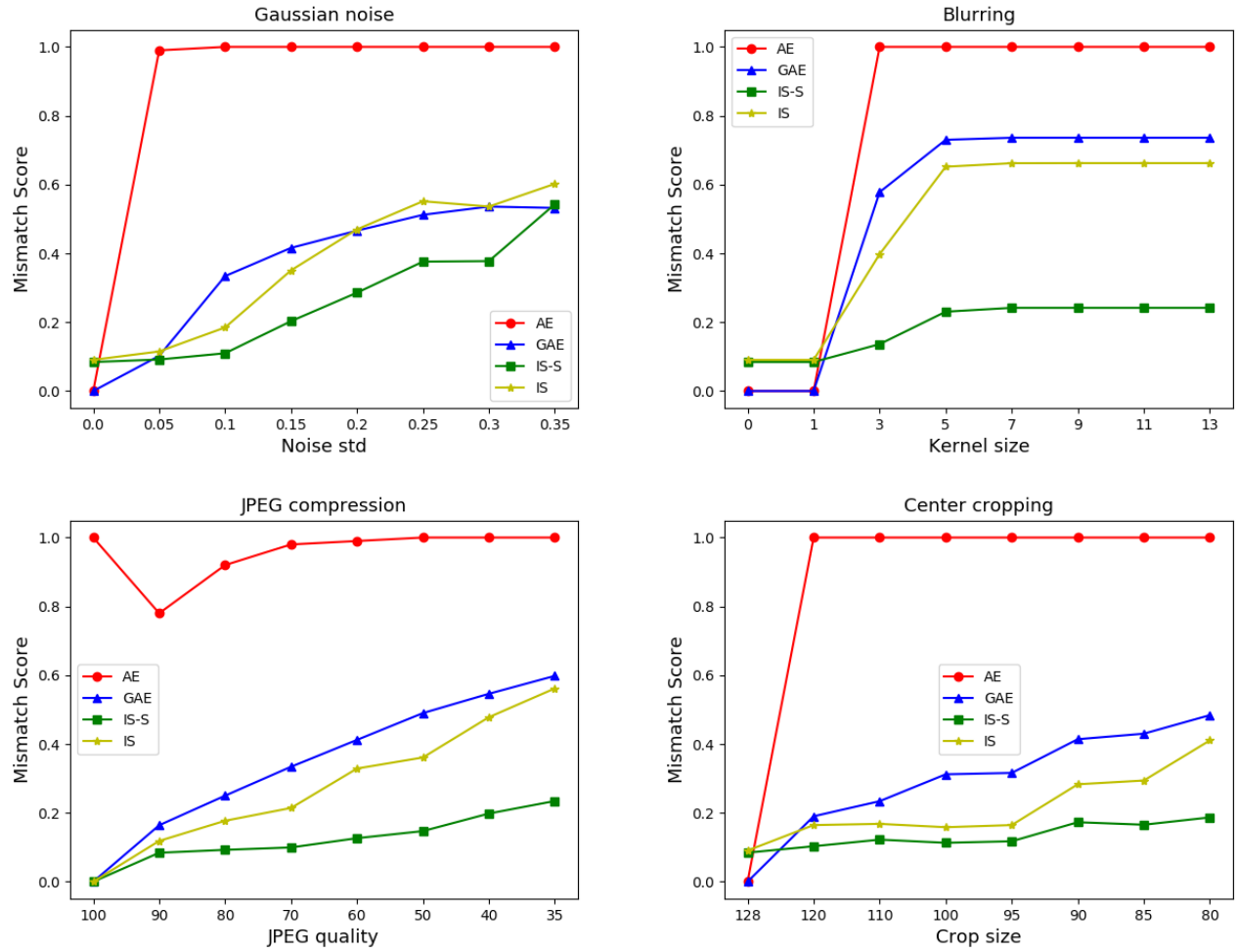


Figure 15: Mismatch Score of STGAN under different settings of transformations, which are applied on the inputs of the GAN.